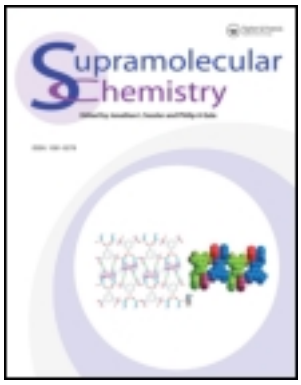

Supramolecular Chemistry
Publication details, including instructions for authors and subscription information:
http://www.tandfonline.com/loi/gsch20

Effects of metal-ligand coordination on the self-assembly behaviour of a crown ether functionalised perylenetetracarboxylic diimide

Ao You [a], Jian Gao [a], Dapan Li [a], Marcel Bouvet [b] & Yanli Chen [a]

[a] Shandong Provincial Key Laboratory of Fluorine Chemistry and Chemical Materials, School of Chemistry and Chemical Engineering, University of Jinan, Jinan, 250022, P.R. China

[b] Institut de Chimie Moléculaire de l'Université de Bourgogne, CNRS UMR 5260, Université de Bourgogne, 21078, Dijon, France

Version of record first published: 18 Oct 2012.

To cite this article: Ao You, Jian Gao, Dapan Li, Marcel Bouvet & Yanli Chen (2012): Effects of metal-ligand coordination on the self-assembly behaviour of a crown ether functionalised perylenetetracarboxylic diimide, Supramolecular Chemistry, 24:12, 851-858

To link to this article: http://dx.doi.org/10.1080/10610278.2012.731063

Supramolecular Chemistry
Vol. 24, No. 12, December 2012, 851–858

Effects of metal–ligand coordination on the self-assembly behaviour of a crown ether functionalised perylenetetracarboxylic diimide

Ao You[a], Jian Gao[a], Dapan Li[a], Marcel Bouvet[b] and Yanli Chen[a]*

[a]*Shandong Provincial Key Laboratory of Fluorine Chemistry and Chemical Materials, School of Chemistry and Chemical Engineering, University of Jinan, Jinan 250022, P.R. China;* [b]*Institut de Chimie Moléculaire de l'Université de Bourgogne, CNRS UMR 5260, Université de Bourgogne, 21078 Dijon, France*

(*Received 21 August 2012; final version received 13 September 2012*)

A novel perylenetetracarboxylic diimide (PDI) derivative, *N*,*N*′-di(4′-benzo-15-crown-5-ether)-1,7-di(4-*tert*-butyl-phenoxy) perylene-3,4;9,10-tetracarboxylic diimide (CRPDI), has been synthesised and characterised. Dimerisation of CRPDI is induced by the presence of K^+ in $CHCl_3$ or spontaneously occurs in methanol, as revealed by absorption and emission spectroscopy. In particular, the formation of co-facial dimer in the presence of K^+ proceeds in a three-stage process, as indicated by absorption spectroscopy. The belt- and rope-like nanostructures of CRPDI fabricated from methanol and $CHCl_3$ solution in the presence of K^+ are obtained by scanning electron microscopy. Furthermore, the conductivity of the rope-like nanostructures from the cation-induced dimeric species is more than ca. 1 order of magnitude higher than the belt-like nanostructures from the solvent-induced dimeric species. The present result represents the further effort towards realisation of controlling and tuning the morphology of self-assembled nanostructures of PDI derivatives through molecular design and synthesis. It will be valuable for the design and preparation of PDI-based nano-(opto)electronic devices with good performance due to the close relationship between the molecular ordering and dimensions of nanostructures and the performance of nanodevices.

Keywords: perylenetetracarboxylic diimide; crown ether; self-assembly; nanostructure; semiconductor

1. Introduction

The construction of organic nano-assembly into a prerequisite structure with controlled morphology by modifying the molecular structure and programming the supramolecular interaction is a great challenge in the field of molecular self-assembly (*1*). The major driving force operating in these precisely controlled nanoscopic architectures arises from various non-covalent interactions including $\pi-\pi$ interaction, van der Waals forces, hydrogen bonding, hydrophilic/hydrophobic interactions, electrostatic and metal–ligand coordination (*2–4*). As a result, comprehensive understanding of the interplay between these factors to create different morphologies has formed the focus of current research interests in this field.

As an important functional dye with outstanding photo and chemical stability, as well as interesting photophysical and photochemical properties, perylenetetracarboxylic diimide (PDI) derivatives have been intensively studied as advanced molecular materials for sensors (*5, 6*), organic solar cell and thin-film transistor applications (*7–9*). For most of the applications, the properties of the molecular materials are closely related to the structure of nano-assembly. Therefore, the fabrication of ordered nanostructures with different morphology of this functional molecular material has become an attracting research area in the past decade (*10–16*). However, crown ethers that have both remarkable recognition and metal-binding properties have wide applications also in molecular electronic devices (*17*). The combination of these two functional subunits for the purpose of constructing novel supramolecular structures would be helpful for improving the semi-conducting properties of some disk-shaped molecules, apparently owing to the increased interaction between adjacent disk-shaped molecules by metal–crown ethers interaction (*18–20*). However, no system that directly exploits intermolecular interactions and corresponding nanostructures based on PDI derivatives containing crown ethers has been reported thus far.

With these ideas in mind, in this paper, we endeavoured to design and synthesise a new PDI compound containing two 4-benzo-15-crown-5-ether units at two imide nitrogen positions of a PDI core, named as *N*,*N*′-di(4′-benzo-15-crown-5-ether)-1,7-di (4-*tert*-butyl-phenoxy)perylene-3,4;9,10-tetracarboxylic diimide (CRPDI; Scheme 1). The self-assembling properties of CRPDI in the absence and presence of potassium ions were comparatively investigated by electronic absorption, fluorescence and scanning electronic microscopy (SEM), revealing the effect of the interaction between potassium ions and crown ether groups on the

*Corresponding author. Email: chm_chenyl@ujn.edu.cn

ISSN 1061-0278 print/ISSN 1029-0478 online

http://dx.doi.org/10.1080/10610278.2012.731063
http://www.tandfonline.com

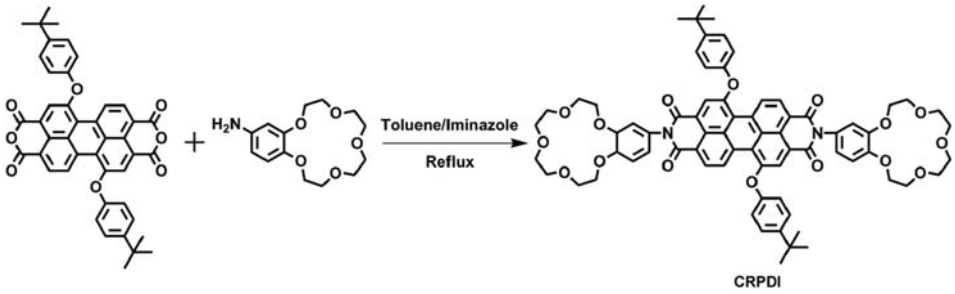

Scheme 1. Synthesis of CRPDI.

morphology and dimension of self-assembled nanostructures. In addition, better semi-conducting properties of the nanostructures fabricated from CRPDI in the presence of potassium ions than those in the absence of potassium ions were also revealed by current–voltage (*I–V*) measurements.

2. Experimental section

2.1. Materials

4-Aminobenzo-15-crown- 5-ether was purchased from Tokyo Chemical Industry Co., Ltd, Tokyo, Japan. All other reagents and solvents were used as received. Column chromatography was carried out on silica gel. 1,7-Di(4-*tert*-butyl-phenoxy)perylene-3,4;9,10-tetracarboxylic dianhydride was prepared following the literature method (*8, 21*).

2.2. General remarks

^{1}H NMR spectra were recorded on a Bruker DPX 400 spectrometer in $CDCl_3$. Spectra were referenced internally using the residual solvent resonance ($\delta = 7.26$ ppm for ^{1}H NMR) relative to $SiMe_4$. MALDI–TOF mass spectra were taken on a Bruker BIFLEX III ultra-high-resolution mass spectrometer with alpha-cyano-4-hydroxycinnamic acid as matrix. Electronic absorption spectra were recorded on a Hitachi U-4100 spectrophotometer. Fluorescence spectra were measured on a K2 system (ISIS product) at room temperature. The fluorescence quantum yields were calculated using *N,N′*-di(cyclohexyl)-1,7-di(4-*tert*-butyl-phenoxy)perylene-3,4;9,10-tetracarboxylic diimide as standard. SEM images were obtained using a JEOL JSM-6700F field-emission SEM. For SEM imaging, Au (1–2 nm) was sputtered onto the substrate to prevent the charging effects and to improve the image clarity. Chemical compositions of the nanostructure were studied by energy-dispersive spectrometry (EDS) with an Oxford INCA X-sight instrument.

2.3. Device fabrication and measurement

The *I–V* characteristics of CRPDI nanostructures fabricated from methanol and $CHCl_3$ solution in the presence of K^+ were obtained with a Keithley 4200 semiconductor characterisation system at room temperature in air. *I–V* curves were registered in the −100 to 100 V voltage range with 1 V increments. All experiments have been repeated for at least twice to ensure reproducibility. The interdigitated electrode array is composed of 10 pairs of indium tin oxide (ITO) electrode digits deposited onto a glass substrate with the following dimensions: 125 μm electrode width, 75 μm spacing, 5850 μm overlapping length and 20 nm electrode thickness. Conductivity, σ, can be calculated by Equation (1) (*21, 22*):

$$\sigma = \frac{dI}{(2n-1) \times L \times h \times V}, \quad (1)$$

where d is the interelectrode spacing, I is the current, n is the number of electrode digits, L is the overlapping length of the electrodes and h is the film thickness if it is less than that of the electrodes or the electrode thickness when the film thickness exceeds that of the ITO electrodes.

2.4. Synthesis and characterisation of CRPDI

A mixture of 1,7-di(4-*tert*-butyl-phenoxy)perylene-3,4;9,10-tetracarboxylic dianhydride (58 mg, 0.08 mmol), 4′-aminobenzo-15-crown-5-ether (90 mg, 0.33 mmol), imidazole 2 g and toluene (10 ml) was heated to 116°C under N_2 atmosphere and continuously stirred for 5 h at this temperature. Then the reaction mixture was cooled to room temperature. After the solvent was evaporated under reduced pressure and the residue was purified by column chromatography on silica gel with 3% MeOH in $CHCl_3$ as eluent, CRPDI (10 mg, yield 10.3%) was collected as bright red solid. MS (m/z): 1221.3 found, 1243.2 ($M^+ + Na^+$), 1259.2($M^+ + K^+$). ^{1}H NMR ($CDCl_3$, 400 MHz): δ 9.62–9.60 (d, 2H), 8.60–8.58 (d, 2H), 8.33 (s, 2H), 7.52–7.45 (m, 4H), 7.12–7.10 (m, 4H), 7.01 (d, 2H), 6.97 (d, 2H), 6.85–6.83 (d, 2H), 4.20 (m, 4H), 4.06 (m, 4H), 3.95 (m, 4H), 3.85 (m, 4H), 3.79–3.77 (m, 16H), 1.37 (s, 18H).

3. Results and discussion

3.1. UV–vis absorption and fluorescence spectra in solution

The electronic absorption and emission spectra of CRPDI in $CHCl_3$ and in the presence of K^+ ions with the concentration ratio of $[K^+]/[CRPDI] = 1$ in this solution are shown in Figure 1, while the corresponding experimental data compiled in Table A1 (Appendix). As expected, CRPDI in chloroform showed typical feature of the diphenoxy-substituted PDI chromophores in the electronic absorption spectra (*8, 23*), revealing the non-aggregated (monomeric) molecular spectroscopic nature of the compound in $CHCl_3$ (Figure 1(A), solid line). In light of the previous observations as reported in the literature with regard to absorption characteristics of similar PDI derivatives (*24–26*), the absorptions at about 551 and 515 nm can be attributed to the 0–0 and 0–1 vibronic band of the $S_0–S_1$ transition, respectively, while the observed absorption band around 407 nm is attributed to the electronic $S_0–S_2$ transition. The fluorescence spectrum of CRPDI in $CHCl_3$ presented as a mirror image of the absorption, which gives no indication of aggregation (Figure 1(B), solid line) (*27*). After potassium ions are added into $CHCl_3$ solution of CRPDI with the concentration ratio of $[K^+]/[CRPDI] = 1$ in this solution, the absorption of CRPDI changed significantly in the ratio of the intensities of the 0–0/0–1 peaks, while peak positions of absorption maxima of CRPDI remained almost unaltered (Figure 1(A), dotted line). With reference to previous spectroscopic work on crown ether appended porphyrin/phthalocyanine analogues (*16, 18, 28–31*), those kinds of changes on the absorption spectra are attributed to the formation of a co-facial and eclipsed configurated species by complexation of the two crown ether units of CRPDI with potassium ions (*16, 32, 33*). In comparison with the fluorescence spectrum of CRPDI in $CHCl_3$, addition of K^+ ions affected CRPDI fluorescence emission by a loss of the fine structures and a broad and structureless emission band with bathochromic shift of about 70 nm (Figure 1(B), dotted line). Such spectral feature are similar to those observed previously for aggregates of core-twisted perylene bisimide dyes (*34*) and can be related to a pronounced structural and energetical relaxation process of the excited dimer aggregate (*35*). Furthermore, the fluorescence quantum yield of CRPDI is reduced from 70.7% for the isolated CRPDI to about 3.54% upon aggregation by using *N*,*N*′-di(cyclohexyl)-1,7-di(4-*tert*-butyl-phenoxy)perylene-3,4;9,10-tetracarboxylic diimide in $CHCl_3$ as a reference (*25, 36*), which is consistent with electronic coupling between a pair (or more) of PDI units formed by the interaction between adjacent CRPDI molecules in the co-facial arrangement (*34, 37*).

3.2. Cation complexation leading to stepwise formation of a co-facial dimeric CRPDI supramolecular structure

The process of K^+-induced co-facial dimer formation from monomeric CRPDI is studied by K^+-triggered spectroscopic evolution of CRPDI in the region of 300–800 nm recorded in $CHCl_3$, as shown in Figure 2. It can be seen that the low-energy 0–0 vibronic band at 551 nm decreases significantly, whereas the high-energy 0–1 band at 515 nm decreases slightly with gradual addition of K^+ ions into solution of CRPDI ($[K^+]/[CRPDI] = 0$ to 2 with a step of 0.2). However, there was a markedly decrease in the ratio of the intensities of the 0–0/0–1 peaks along with an increase of $[K^+]/[CRPDI]$ in solution, indicating that the addition of K^+ is giving rise to co-facial dimer formation (*16, 37*). As seen from the inset of Figure 2, from about $[K^+]/[CRPDI] = 1$ onward, the ratio of the intensities of the 0–0/0–1 peaks remains unchanged, indicating that the aggregation process reaches a steady state.

The co-facial dimer formation was monitored by variation of the absorbance at 515 nm (the so-called dimer band) and 551 nm (monomer band) of CRPDI during the

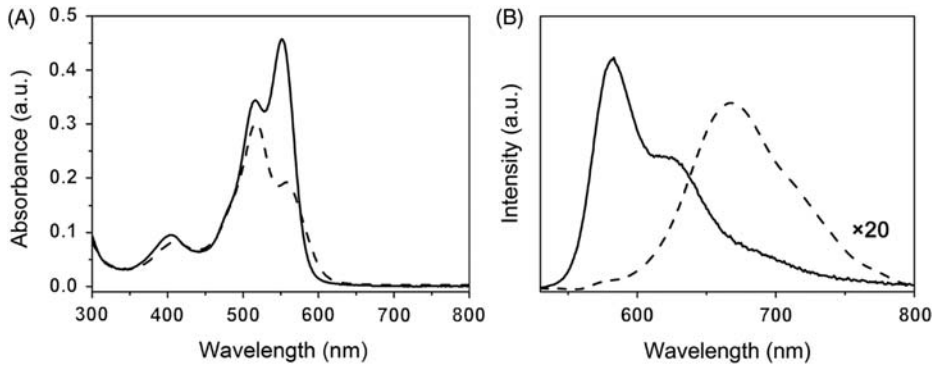

Figure 1. UV–vis absorption (A) and fluorescence (B) spectra of CRPDI in 0.01 mM chloroform solution (solid line) and after addition of K^+ ions (KOAc) with the concentration ratio of $[K^+]/[CRPDI] = 1$ in this solution (dotted line). The excited wavelength was 515 nm.

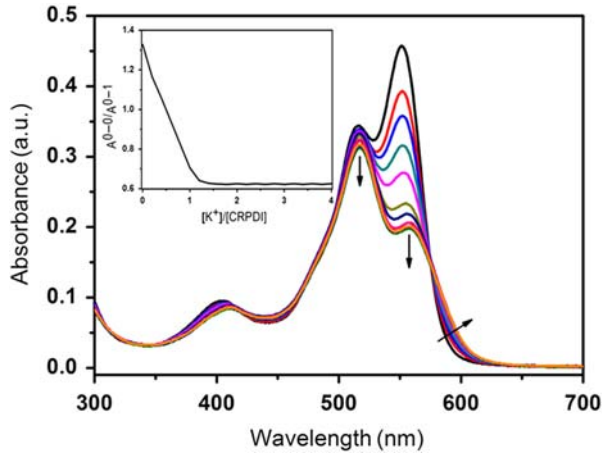

Figure 2. Absorption spectra of CRPDI with various mole ratios of K^+ ions. A solution of KOAc (1 mM) in $CHCl_3/CH_3OH$ (95:5 v/v) was added gradually to a solution of CRPDI (0.01 mM, 3 ml) in $CHCl_3$. The arrows indicate the direction of the spectroscopic change from progressively increasing the concentration ratio of K^+ ions to CRPDI: $[K^+]/[CRPDI]$ from 0 to 2 with a step of 0.2. Inset shows the changes in the ratio of vibronic bands A^{0-0}/A^{0-1} of CRPDI with various mole rations of K^+ ions.

addition of KOAc in $CHCl_3/CH_3OH$ (95:5 v/v). As can be seen from Figure 3, the reversed change of the relative intensity of two characteristic bands indicates that upon addition of K^+ ions, monomer (CRPDI) is converted into the dimeric supermolecular structure (CRPDI–K_n^+–CRPDI), in which K^+ ions are sandwiched between two crown ether units belonging to two different CRPDIs. In this case, the process of K^+-induced dimerisation of CRPDI is proposed in the following three stages (*18, 38*): firstly, two monomeric 15-crown-5-substituted PDI molecules combine with the first K^+ ion to form a eclipsed and/or linear (non-co-facial) dimer in the region of $0 < [K^+]/[CRPDI] \leq 0.5$; secondly, in the region of

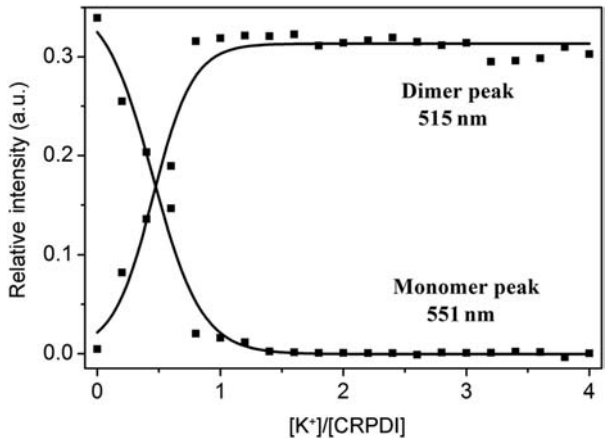

Figure 3. Variation of the absorbance at 515 and 551 nm of CRPDI during addition of KOAc in $CHCl_3/CH_3OH$ (95:5 v/v).

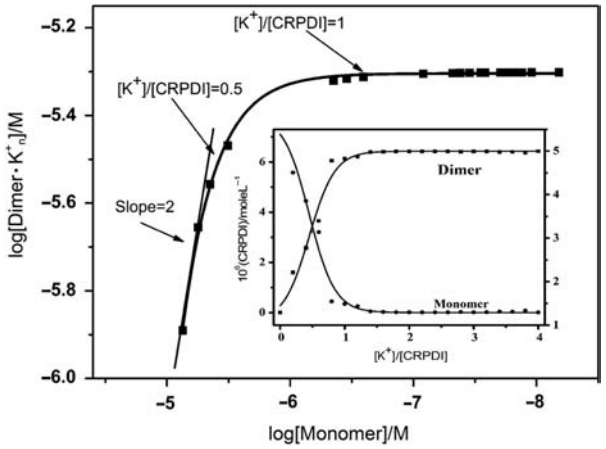

Figure 4. Plot of log [monomer] vs. log [dimer·K_n^+] in $CHCl_3/CH_3OH$. The inset shows the dependence of monomer and dimer concentrations on $[K^+]/[CRPDI]$.

$0.5 < [K^+]/[CRPDI] \leq 1$ the transition from a non-co-facial dimer to a co-facial dimer conducts by binding the second K^+ ion; finally, the change reached saturation at $[K^+]/[CRPDI] \geq 1$, the complete formation of a co-facial dimer is achieved. In other words, the first stage dimer is non-co-facial while the final dimer is a co-facial species.

$$n\mathrm{K}^+ + 2\,\mathrm{monomer\,(CRPDI)} \overset{\mathrm{K}}{\longleftrightarrow} \mathrm{dimer}\cdot\mathrm{K}_n^+(\mathrm{CRPDI} - \mathrm{K}_n^+ - \mathrm{CRPDI}). \quad (2)$$

Equation (2) is proposed with the speculation that the equilibrium between monomer CRPDI (upon addition of K^+ ions) and the corresponding dimer (CRPDI–K_n^+ – CRPDI) should exist in the present system. The monomer and dimer concentrations could be calculated from the spectral changes during titration using the method described by West and Pearce (*39*). If Equation (2) was available, the slope of 2 from a plot of log [monomer] versus log [dimer·K_n^+] would be obtained. As expected, the region with a slope of ca. 2.0 is revealed in Figure 4. When K^+ ions are added to the CRPDI solution, the monomer concentration decreases sharply, and a region with slope ≈ 2.0 continues until $[K^+]/[CRPDI] = 0.5$. After this point, the slope of the plot approaches 0, especially beyond the region $[K^+]/[CRPDI] > 1$ (*18*). Furthermore, a very high binding constant, $K = (1.76 \pm 0.02) \times 10^{11}\,\mathrm{l^2\,mol^{-2}}$, for Equation (2) with $n = 1$ is obtained when two CRPDI units bind one K^+ cation and start to form the dimer in the first stage (*18, 19*).

3.3. *Optical properties in the solid state*

The aggregation behaviour of CRPDI in solid state was studied by UV–vis and fluorescence spectroscopy.

Two kinds of solid films were prepared from the evaporation of a drop of CRPDI solution in $CHCl_3$ with or without K^+($[K^+]/[CRPDI] = 1$) on the quartz substrates for analysis, named film **1** and **2**, respectively. For comparison, the solids that precipitated by injecting a small volume of solution of CRPDI in $CHCl_3$ solution (1 mM) into a large volume of methanol were transferred to a quartz substrate (film **3**). In comparison with the absorption spectrum of CRPDI in $CHCl_3$, obvious band broadening was observed in films **1**–**3** (Figure 5(A)) due to the effect of the closely compacted molecular assembly. Furthermore, the relative enhancement of the 0–1 transition in the order of film **2** > film **3** > film **1** was revealed by the normalised absorption spectra, which implied the formation of H-type aggregation in films **1**–**3**, and in particular the increasing excitonic interactions between the stacked CRPDI chromophores in the same order (*37, 40, 41*). Consistent with the absorption measurement, all the fluorescence spectra in the films **1**–**3** showed a new emission at about 694 nm for film **1** and 698 nm for films **2**–**3**, respectively (Figure 5(B), Appendix, Table A1), which is a typical emission of PDI excimer-like state, suggesting strong $\pi-\pi$ stacking and a typical H-type aggregation configuration (*32, 42, 43*).

3.4. *Morphology of the aggregates*

The morphology of the films **1**–**3** formed from CRPDI was examined by SEM. As seen from Figure 6, the CRPDI aggregate morphology shows either cation- or solvent-dependent variation. Film **1** prepared from evaporation of a drop of CRPDI solution in $CHCl_3$ results in disordered flake aggregates on the surface of this film (Figure 6(A)). After the addition of K^+ ions in CRPDI solution with $[K^+]/[CRPDI] = 1$, due to metal–ligand (15C5–K^+–15C5) coordination between neighbouring CRPDI molecules in cooperation with intermolecular $\pi-\pi$ interaction, CRPDI molecules assembled into nanostructures with long 1D rope-like bundles. As shown in Figure 6(B), long 1D nanoropes display uniform orientation and size with an average width of ca. 75 nm and a length of over 2 μm. The success in preparing ordered 1D nanoropes from CRPDI by introducing potassium ions (KOAc) was confirmed by the elemental signatures of C, O, N and K in EDS as shown in the inset of Figure 6(B). CRPDI molecules precipitated from methanol result in belt-like nanostructures with an average width of 200 nm and length of ca. 5 μm. The obvious difference on the morphology of films **1**–**3** of CRPDI indicates the effect of a synergistic interplay among non-covalent interactions, including $\pi-\pi$ interaction, metal–ligand coordination and the interactions between CRPDI molecules and solvent on fine controlling and tuning the molecular packing conformation of the corresponding self-assembled aggregates. It is worth note that the size- and morphology-adjustable nanostructures are highly desired for fabricating nanoscale molecular (opto)-electronic devices which often require a wide variety of channel lengths to achieve the optimum gate or optical modulation (*3, 44*).

3.5. **I–V** *properties*

The uniform aggregates of CRPDI with well-defined nanostructures would be promising candidates for applications in electronic devices. To demonstrate the potentials of these nanostructures, thin films of **1**–**3** of CRPDI were carefully prepared onto glass substrates with ITO interdigitated electrode structures, respectively. After complete evaporation of the solvents, the densely packed nanostructures (films) remained and adhere to ITO interdigitated electrodes (IDEs)/glass substrate tightly, and the electron conductivity was measured. Figure 7 shows the *I*–*V* characteristics of nanoropes and nanobelts from CRPDI. According to the equation reported in the literatures (*21, 22*), the electronic conductivity is calculated to be around 2.6×10^{-5} and 3.5×10^{-6} S cm^{-1} for the

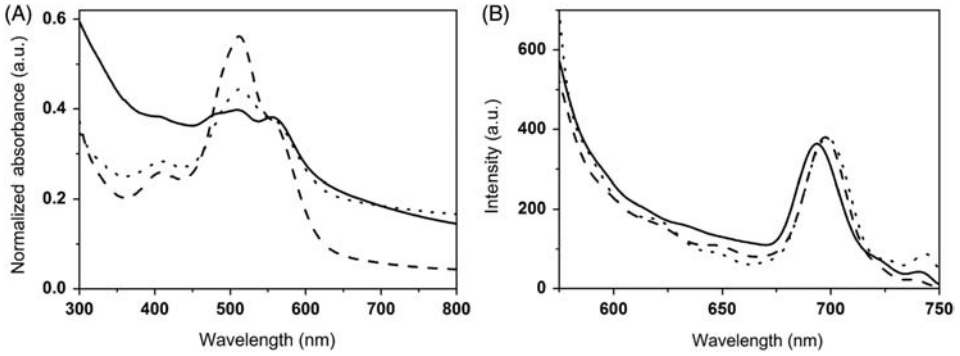

Figure 5. UV–vis absorption (A) and fluorescence (B) spectra of CRPDI films prepared from evaporation of a drop of CRPDI solution in $CHCl_3$ on a quartz substrate (solid line), and in the presence of K^+ ions in this solution with $[K^+]/[CRPDI] = 1$ on a quartz substrate (dashed line), CRPDI solids precipitated from methanol (dotted line). The excited wavelength was 515 nm. The absorption spectra are normalised at 515 nm.

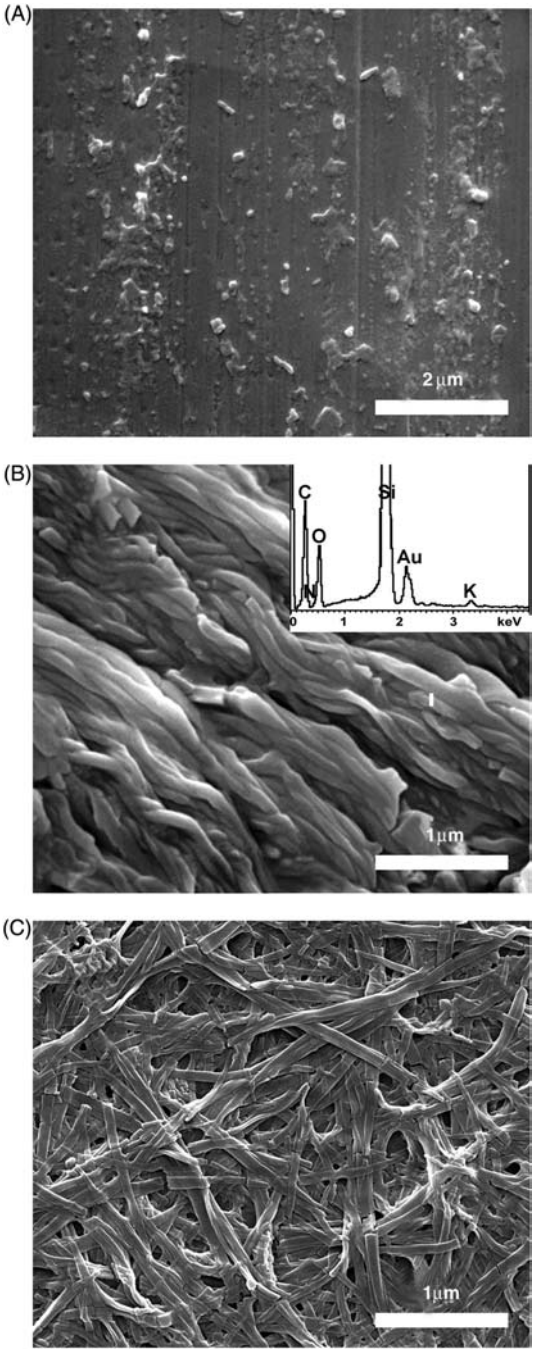

Figure 6. SEM images of CRPDI solids prepared from evaporation of a drop of CRPDI solution in $CHCl_3$ on a quartz substrate (A), and after addition of K^+ ions in this solution with $[K^+]/[CRPDI] = 1$ on a quartz substrate (B), CRPDI solids precipitated from methanol (C). The inset of Figure 6(B) shows the energy-dispersive analysis of a single nanorope of CRPDI.

nanoropes (film **2**) and nanobelts (film **3**) of CRPDI, respectively (the experiments were repeated for more than two times on different pieces of films). However, no valuable $I-V$ curve from film **1** (CRPDI aggregates formed in chloroform solution) was obtained due to its disordered

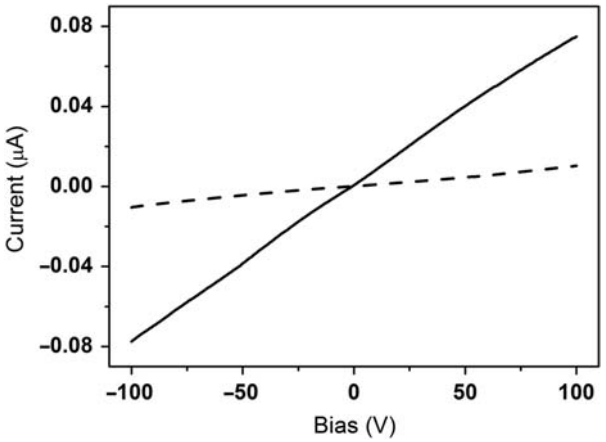

Figure 7. $I-V$ curves measured on nanoropes (solid line) and nanobelts (dashed line) from CRPDI.

structure. Comparing with nanobelts for CRPDI, the improved conductivity of nanoropes for CRPDI might be attributed to both readily π-stacks with adjacent planar molecules and higher ordered molecular arrangement (*24, 45*). The fewer traps and/or defects in these 1D aggregates with more efficient $\pi-\pi$ stacks and metal–ligand coordination interactions should favour charge transport. These aggregates with high current modulation could be useful for a wide range of electronic and sensor devices. In order to evaluate the effect of adding one molar equivalent of KOAc itself and the effect of using different casting solvents ($CHCl_3$ vs. methanol), the $I-V$ characteristics of two kinds of thin films (films **4** and **5**) of a non-crown ether-functionalised PDI derivative [*N*,*N*′-di(cyclohexyl)-1,7-di(4-*tert*-butyl-phenoxy)perylene-3,4;9,10-tetracarboxylic diimide (CHPDI, Appendix, Scheme A1)] were investigated comparatively. Film **4** was prepared by drop-casting from CHPDI solution in $CHCl_3$ with KOAc ($[K^+]/[CHPDI] = 1$), whereas film **5** by transferring the solids that precipitated from methanol. Only valuable $I-V$ curve was obtained from film **5** (Appendix, Figure A1). This result further proved that the addition of the K^+ improved the aggregates of CRPDI due to efficient metal–ligand coordination interactions between CRPDI molecules.

4. Conclusions

We have synthesised a novel PDI with two benzo-15-crown-5 substituents at the two imide nitrogen positions, CRPDI. The aggregation properties were investigated. The co-facial dimeric supramolecular structures of this molecule in the presence of K^+ is formed through a two-step three-stage process in $CHCl_3$. Aggregates with distinct morphologies and nanostructures for CRPDI were controllably prepared by the addition of K^+ or changing the solvent. The $I-V$ measurements on these

molecular aggregates revealed that the present CRPDI molecule might serve as the useful functional materials for nano-electronics.

Acknowledgements

Financial support from the Natural Science Foundation of China (20871055), Natural Science Foundation of Shandong Province (ZR2011BZ005) and University of Jinan in China is gratefully acknowledged.

References

(1) Hoeben, F.J.M.; Jonkheijm, P.; Meijer, E.W.; Schenning, A.P.H.J. *Chem. Rev.* **2005**, *105*, 1491–1546.
(2) Elemans, J.A.A.W.; van Hameren, R.; Nolte, R.J.M.; Rowan, A.E. *Adv. Mater.* **2006**, *18*, 1251–1266.
(3) Lu, G.; Chen, Y.; Zhang, Y.; Bao, M.; Bian, Y.; Li, X.; Jiang, J. *J. Am. Chem. Soc.* **2008**, *130*, 11623–11630.
(4) (a) Ajayaghosh, A.; Praveen, V.K. *Acc. Chem. Res*. **2007**, *40*, 644–656; (b) Ajayaghosh, A.; Chithra, P.; Varghese, R. *Angew. Chem.* **2007**, *46*, 230–233; (c) Chithra, P.; Varghese, R.; Divya, K. P.; Ajayaghosh, A. *Chem. Asian J*. **2008**, *3*, 1365–1373.
(5) Che, Y.; Yang, X.; Loser, S.; Zang, L. *Nano Lett.* **2008**, *8*, 2219–2223.
(6) Naddo, T.; Che, Y.; Zhang, W.; Balakrishnan, K.; Yang, X.; Yen, M.; Zhao, J.; Moore, J.S.; Zang, L. *J. Am. Chem. Soc.* **2007**, *129*, 6978–6979.
(7) Zhao, L.; Ma, T.; Bai, H.; Lu, G.; Li, C.; Shi, G. *Langmuir* **2008**, *24*, 4380–4387.
(8) Wang, Y.; Chen, Y.; Li, R.; Wang, S.; Su, W.; Ma, P.; Wasielewski, M.R.; Li, X.; Jiang, J. *Langmuir* **2007**, *23*, 5836–5842.
(9) Oh, J.H.; Liu, S.; Bao, Z.; Schmidt, R.; Würthner, F. *Appl. Phys. Lett.* **2007**, *91*, 212107-1–212107-3.
(10) Balakrishnan, K.; Datar, A.; Oitker, R.; Chen, H.; Zuo, J.; Zang, L. *J. Am. Chem. Soc.* **2005**, *127*, 10496–10497.
(11) Balakrishnan, K.; Datar, A.; Naddo, T.; Huang, J.; Oitker, R.; Yen, M.; Zhao, J.; Zang, L. *J. Am. Chem. Soc.* **2006**, *128*, 7390–7398.
(12) Sinks, L.E.; Rybtchinski, B.; Iimura, M.; Jones, B.A.; Goshe, A.J.; Zuo, X.; Tiede, D.M.; Li, X.; Wasielewski, M.R. *Chem. Mater.* **2005**, *17*, 6295–6303.
(13) Gesquière, A.; Jonkheijm, P.; Hoeben, F.J.M.; Schenning, A.P.H.J.; De Feyter, S.; De Schryver, F.C.; Meijer, E.W. *Nano Lett.* **2004**, *4*, 1175–1179.
(14) Xu, S.; Sun, J.; Ke, D.; Song, G.; Zhang, W.; Zhan, C. *J. Colloid Interface Sci.* **2010**, *349*, 142–147.
(15) Schenning, A.P.H.J.; v. Herrikhuyzen, J.; Jonkheijm, P.; Chen, Z.; Würthner, F.; Meijer, E.W. *J. Am. Chem. Soc.* **2002**, *124*, 10252–10253.
(16) Yang, X.; Xu, X.; Ji, H.-F. *J. Phys. Chem. B* **2008**, *112*, 7196–7202.
(17) Engelkamp, H.; Nolte, R.J.M. *J. Porphyrins Phthalocyanines* **2000**, *4*, 454–459.
(18) Kobayashi, N.; Lever, A.B.P. *J. Am. Chem. Soc.* **1987**, *109*, 7433–7441.
(19) Sielcken, O.E.; Van Tilborg, M.M.; Roks, M.F.M.; Hendriks, R.; Drenth, W.; Nolte, R.J.M. *J. Am. Chem. Soc.* **1987**, *109*, 4261–4265.
(20) Sheng, N.; Li, R.; Choi, C.-F.; Su, W.; Ng, D.K.P.; Cui, X.; Yoshida, K.; Kobayashi, N.; Jiang, J. *Inorg. Chem.* **2006**, *45*, 3794–3802.
(21) Zhao, C.; Zhang, Y.; Li, R.; Li, X.; Jiang, J. *J. Org. Chem.* **2007**, *72*, 2402–2410.
(22) Ahn, H.; Chandekar, A.; Kang, B.; Sung, C.; Whitten, J.E. *Chem. Mater.* **2004**, *16*, 3274–3278.
(23) Chen, Y.; Bouvet, M.; Sizun, T.; Gao, Y.; Plassard, C.; Lesniewska, E.; Jiang, J. *Phys. Chem. Chem. Phys.* **2010**, *12*, 12851–12861.
(24) Chen, Y.; Feng, Y.; Gao, J.; Bouvet, M. *J. Colloid Interface Sci.* **2012**, *368*, 387–394.
(25) Würthner, F.; Thalacker, C.; Diele, S.; Tschierske, C. *Chem. Eur. J.* **2001**, *7*, 2245–2253.
(26) Wasielewski, M.R. *Acc. Chem. Res.* **2009**, *42*, 1910–1921.
(27) Chen, Y.; Chen, L.; Qi, G.; Wu, H.; Zhang, Y.; Xue, L.; Zhu, P.; Ma, P.; Li, X. *Langmuir* **2010**, *26*, 12473–12478.
(28) Kobayashi, N.; Togashi, M.; Osa, T.; Ishii, K.; Yamauchi, S.; Hino, H. *J. Am. Chem. Soc.* **1996**, *118*, 1073–1085.
(29) Thanabal, V.; Krishnan, V. *J. Am. Chem. Soc.* **1982**, *104*, 3643–3650.
(30) van Willigen, H.; Chandrashekar, T.K.; Das, U.; Ebersole Marie, H. *Electron Paramagnetic Resonance Study of Dimerization Effects on Porphyrins in the Photoexcited Triplet State*; American Chemical Society: Washington, DC, 1986; p. 140–153.
(31) Chitta, R.; Rogers, L.M.; Wanklyn, A.; Karr, P.A.; Kahol, P.K.; Zandler, M.E.; D'Souza, F. *Inorg. Chem.* **2004**, *43*, 6969–6978.
(32) Wu, H.; Xue, L.; Shi, Y.; Chen, Y.; Li, X. *Langmuir* **2011**, *27*, 3074–3082.
(33) Xue, L.; Wu, H.; Shi, Y.; Liu, H.; Chen, Y.; Li, X. *Soft Matter* **2011**, *7*, 6213–6221.
(34) Chen, Z.; Baumeister, U.; Tschierske, C.; Würthner, F. *Chem. Eur. J* **2007**, *13*, 450–465.
(35) Birks, J.B. *Rep. Prog. Phys.* **1975**, *38*, 903–974.
(36) Xue, L.; Wang, Y.; Chen, Y.; Li, X. *J. Colloid Interface Sci.* **2010**, *350*, 523–529.
(37) Neelakandan, P.P.; Pan, Z.; Hariharan, M.; Zheng, Y.; Weissman, H.; Rybtchinski, B.; Lewis, F.D. *J. Am. Chem. Soc.* **2010**, *132*, 15808–15813.
(38) Sheng, N.; Zhang, Y.; Xu, H.; Bao, M.; Sun, X.; Jiang, J. *Eur. J. Inorg. Chem.* **2007**, *20*, 3268–3275.
(39) West, W.; Pearce, S. *J. Phys. Chem.* **1965**, *69*, 1894–1903.
(40) An, Z.; Yu, J.; Jones, S.C.; Barlow, S.; Yoo, S.; Domercq, B.; Prins, P.; Siebbeles, L.D.A.; Kippelen, B.; Marder, S.R. *Adv. Mater.* **2005**, *17*, 2580–2583.
(41) Giaimo, J.M.; Gusev, A.V.; Wasielewski, M.R. *J. Am. Chem. Soc.* **2002**, *124*, 8530–8531.
(42) Würthner, F.; Chen, Z.; Dehm, V.; Stepanenko, V. *Chem. Commun.* **2006**, 1188–1190.
(43) Ma, Y.; Wang, C.; Zhao, Y.; Yu, Y.; Han, C.; Qiu, X.; Shi, Z. *Supramol. Chem.* **2007**, *19*, 141–149.
(44) Babel, A.; Jenekhe, S.A. *J. Am. Chem. Soc.* **2003**, *125*, 13656–13657.
(45) Rella, R.; Serra, A.; Siciliano, P.; Tepore, A.; Valli, L.; Zocco, A. *Langmuir* **1997**, *13*, 6562–6567.

Appendix A

Table A1. Peak positions of absorption (λ_a) and emission (λ_e) maxima for CRPDI in chloroform and in the presence of K^+ ions with the concentration ratio of $[K^+]/[CRPDI] = 1$ in this solution together with CRPDI films prepared from evaporation of a drop of CRPDI solution in $CHCl_3$ on a quartz substrate (film **1**), and after the addition of K^+ ions in this solution with $[K^+]/[CRPDI] = 1$ on a quartz substrate (film **2**), CRPDI films precipitated from methanol (film **3**).

CRPDI	λ_a (nm)	λ_e (nm)
Solution in $CHCl_3$	407, 515, 551	584
Solution with $[K^+]/[CRPDI] = 1$	411, 517, 557	668
Film **1**	408, 504, 552	694
Film **2**	408, 508, 553	698
Film **3**	409, 508, 554	698

Note: The excited wavelength was 515 nm.

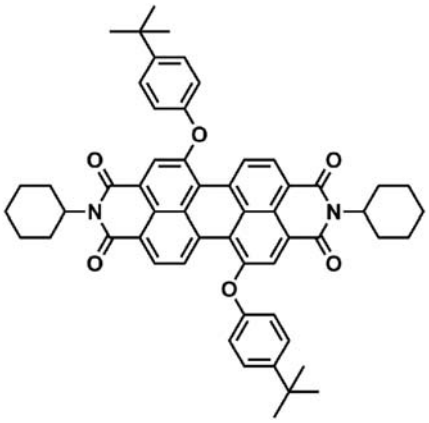

Scheme A1. Schematic structures of CHPDI.

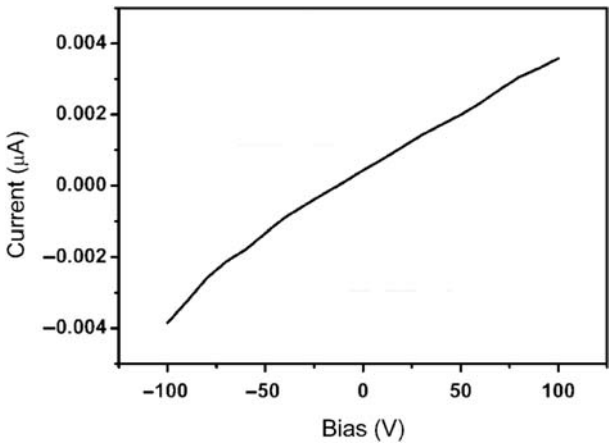

Figure A1. *I–V* curve measured on film **5** of CHPDI from methanol.